Substrate Elastic Modulus Regulates the Morphology, Focal Adhesions, and alpha-Smooth Muscle Actin Expression of Retinal Muller Cells

Bu, Shao-Chong; Kuijer, Roel; van der Worp, Roelofje J.; van Putten, Sander M.; Wouters, Olaf; Li, Xiao-Rong; Hooymans, Johanna M. M.; Los, Leonoor I.

Published in:
Investigative ophthalmology & visual science

DOI:
10.1167/iovs.14-15969

Publication date:
2015

Substrate Elastic Modulus Regulates the Morphology, Focal Adhesions, and α-Smooth Muscle Actin Expression of Retinal Müller Cells

Shao-Chong Bu,[1–3] Roel Kuijer,[2,4] Roelofje J. van der Worp,[1,2] Sander M. van Putten,[2,5] Olaf Wouters,[2,5] Xiao-Rong Li,[3] Johanna M. M. Hooymans,[1,2] and Leonoor I. Los[1,2]

[1]Department of Ophthalmology, University of Groningen, University Medical Center Groningen, Groningen, The Netherlands
[2]W.J. Kolff Institute, Graduate School of Medical Sciences, University of Groningen, Groningen, The Netherlands
[3]Tianjin Medical University Eye Centre, Tianjin Medical University, Tianjin, China
[4]Department of Biomedical Engineering-FB40, University of Groningen, University Medical Center Groningen, Groningen, The Netherlands
[5]Department of Pathology and Medical Biology, University Medical Center Groningen, University of Groningen, Groningen, The Netherlands

Correspondence: Leonoor I. Los, University Medical Center Groningen, Department of Ophthalmology-BB 61, PO Box 30.001, 9700 RB, Groningen, The Netherlands; l.i.los@umcg.nl.

Submitted: October 30, 2014
Accepted: August 4, 2015

Citation: Bu S-C, Kuijer R, van der Worp RJ, et al. Substrate elastic modulus regulates the morphology, focal adhesions, and α-smooth muscle actin expression of retinal Müller cells. *Invest Ophthalmol Vis Sci*. 2015;56:5974–5982. DOI:10.1167/iovs.14-15969

Purpose. The stiffness of the extracellular matrix has been shown to regulate cell adhesion, migration, and transdifferentiation in fibrotic processes. Retinal Müller cells have been shown to be mechanosensitive; they are involved in fibrotic vitreoretinal diseases. Since fibrosis increases the rigidity of the extracellular matrix, our aim was to develop an in vitro model for studying Müller cell morphology and differentiation state in relation to matrix stiffness.

Methods. A spontaneously immortalized human Müller cell line (MIO-M1) was cultured on type I collagen–coated polyacrylamide gels with Young's moduli ranging from 2 to 92 kPa. Cell surface area, focal adhesion, and the expression and morphology of α-smooth muscle actin induced by transforming growth factor β (TGF-β [10 ng/mL for 48 hours]) were analyzed by immunocytology. The images were documented by using fluorescence microscopy and confocal scanning laser microscopy.

Results. MIO-M1 cells cultured on stiff substrates exhibited a significant increase in cell surface area, stress fiber, and mature focal adhesion formation. Furthermore, Müller cells treated with TGF-β1 and TGF-β2 and cultured on stiff substrates showed an increased incorporation of α-smooth muscle actin into stress fibers when compared to those grown on soft surfaces.

Conclusions. Compliance of the surrounding matrix seems to influence the morphology and contraction of retinal Müller cells in fibrotic conditions. Development of an in vitro model simulating both the normally compliant retinal tissue and the rigid retinal fibrotic tissue helps fill the gap between the results of petri-dish cell culture with rigid surfaces and in vivo findings.

Keywords: Müller cells, substrate elastic modulus, mechanosensing, focal adhesion, transforming growth factor

Despite advances in modern surgical techniques, the fibrocontractive vitreoretinal diseases—including proliferative vitreoretinopathy, proliferative diabetic retinopathy, and idiopathic or secondary macular epiretinal membrane (ERM)—remain the major causes of irreversible damage to visual functioning.[1] The resultant preretinal fibrocellular membranes consist of rigid and contractile scar tissue containing excessive fibrotic collagen deposition and contractile myofibroblasts.[2] The formation of the fibrocontractive membrane is considered to represent a fibrotic process, in which myofibroblasts are actively involved.[3] This membrane will distort retinal anatomy, lead to disruption of the photoreceptor cells, to formation of rigid retinal folds, and to recurrent tractional retinal detachment.

The myofibroblast is a crucial cell type in wound healing and fibrotic processes because of its amply clarified function of extracellular matrix protein (mainly collagens) secretion and tissue contraction. In normal wound healing, myofibroblasts usually undergo apoptosis when the wound is healed. In fibrotic diseases, myofibroblasts are persistently activated, resulting in excessive deposition of collagens and severe tissue contraction.[4] The formation and persistence of myofibroblasts are driven by many profibrotic cytokines and growth factors. Transforming growth factor β (TGF-β) remains the most potent inducer of myofibroblast formation.[5] Recent studies[6–9] suggest that matrix stiffness, a measure of matrix resistance to mechanical deformation, regulates TGF-β–induced myofibroblast formation in a wide range of fibrotic processes in heart, lung, liver, and ocular tissue. These findings indicate that the increased matrix stiffness caused by the fibrotic process itself will promote myofibroblast formation and thus will further stimulate the fibrotic process.

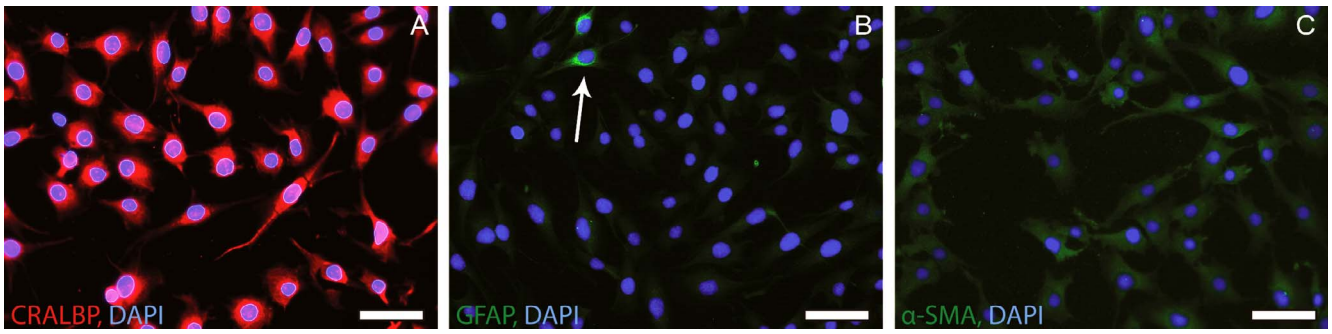

Figure 1. MIO-M1 cells (passage 62) grown for 48 hours on noncoated plastic tissue culture surfaces, using routine stock medium with 10% fetal bovine serum. (**A**) All Müller cells were stained with anti-CRALBP antibody (CRALBP, *red*). (**B**) Only a few MIO-M1 cells were stained with GFAP antibody (GFAP, *green*, *arrow*). (**C**) All MIO-M1 cells show diffuse staining for α-SMA, (α-SMA, *green*) but no α-SMA stress fibers. *Scale bars*: 100 μm.

The fibrocontractive vitreoretinal diseases are associated with TGF-β–induced myofibroblast formation and tissue stiffening, which indicates that the increase in the elastic modulus of the tissue may play a role in the formation of retinal fibrosis.[10–14] Quiescent cells, normally present in vitreous and retina—including hyalocytes, retinal pigment epithelial cells, and retinal glial cells—have been shown to be able to transdifferentiate into a myofibroblast-like cell type characterized by the expression of α-smooth muscle actin (α-SMA).[15–18] Among the retinal glial cells, the retinal Müller cell is one of the major cell types involved in the formation of an ERM, and it can transdifferentiate into an α-SMA–expressing phenotype resulting in ERM contraction.[2,19,20] The primary location of the retinal Müller cell is in the retina, with a very compliant surrounding extracellular matrix. Previous studies have described retinal Müller cells in situ expressing cellular retinaldehyde-binding protein (CRALBP), no α-SMA, and only limited amounts of glial fibrillary acidic protein (GFAP).[21,22] The latter is upregulated in conditions of Müller cell activation.[23] However, when retinal Müller cells migrate to the site of ERM formation, they will encounter a stiffer matrix.[24] Evidence suggests that retinal Müller cells can sense the stiffness of the matrix and alter their cytoskeleton and gene expression profile accordingly.[25] Furthermore, outside-in traction forces have been shown to induce activation of retinal Müller cells in an ex vivo animal model.[26] However, the molecular mechanisms and the effects of substrate elastic modulus on TGF-β responsiveness in retinal Müller cells remain unclear.

We hypothesized that retinal Müller cells are mechanosensitive and that their responsiveness to TGF-β is regulated by the substrate elastic modulus of the supporting matrix. Thus, they may contribute to the initiation and progression of retinal fibrotic diseases. We therefore studied the effects of TGF-β and substrate stiffness in a spontaneously immortalized retinal Müller cell line.

Materials and Methods

Culture of Müller Cells

The MIO-M1 cell line is a spontaneously immortalized human retinal Müller cell line, which was kindly provided by G. Astrid Limb (Moorfields/Institute of Ophthalmology, London, UK). The MIO-M1 cells retained some important characteristics of Müller cells in situ.[27] At the start of each experiment we checked and confirmed that MIO-M1 cells were positive for CRALBP and expressed only very limited amounts of GFAP (Fig. 1A, 1B).

Dulbecco's modified Eagle's medium with high glucose–containing glutaMAX-I (Life Technologies, Inc., Rockville, MD, USA), supplemented with 1% penicillin/streptomycin, was the stock medium. The stock culture of MIO-MI (passage between 60 and 70) was maintained in this medium, with an additional 10% fetal bovine serum (FBS; Life Technologies, Inc.), at 37°C with 5% CO_2, for the purpose of our experiments.

Tunable Polyacrylamide Gels (PAGs), Preparation and Characterization

Polyacrylamide gels with tunable elasticity were prepared on glass coverslips (15 mm; VWR, Radnor, PA, USA) according to the protocol of Pelham and Wang,[28,29] as described previously, with some modifications. The coverslips were soaked in 99% pure ethanol containing 0.5% 3-(trimethoxysilyl) propyl methacrylate and 0.3% acetic acid for 3 minutes. Then the coverslips were rinsed with 99% pure ethanol and stored in 99% ethanol for later use. A 20 × 30-cm glass plate coated with dichlorodimethylsilane was used as the polymerization surface. The gel mixtures were composed of 7.5% acrylamide, 0.01% to 0.3% bisacrylamide (bis; Bio-Rad Laboratories, Hercules, CA, USA), 0.1% ammonium persulfate, and 0.2% N, N, N′,N′-tetramethylethylenediamine (TEMED; Sigma-Aldrich Corp., St. Louis, MO, USA), which were diluted in a 10-mM 4-(2-hydroxyethyl)-1-piperazineethanesulfonic acid (HEPES; Life Technologies, Carlsbad, CA, USA) buffered solution (pH 8). Afterwards, a 100-μL aliquot was placed on the glass plate and a coverslip was placed on top of the droplet. The desired elasticity of the PAGs was achieved by varying the percentage of acrylamide and bis. Elastic moduli ranged from 2 to 92 kPa to model the elastic modulus range that the Müller cells may encounter at the vitreoretinal interface (neural retina: 1–20 kPa[13,30]; vitreal side of retinal inner limiting membrane: approximately 44 kPa[31]). Polyacrylamide gels were polymerized on a coverslip for 30 minutes and removed from the glass plate. Then they were incubated with a cross-linker to ligate collagens to the PAGs. After washing three times with sterile phosphate-buffered saline (PBS), the PAGs were functionalized by incubation with 30 μg/mL type I collagen (Advanced BioMatrix, San Diego, CA, USA), diluted in PBS at 37°C for 2 hours and rinsed with PBS afterwards. The final thickness of the PAGs was approximately 100 μm. The PAGs on the coverslips were placed in 6-well culture plates, filled with 2 mL PBS and stored at 4°C. The validation of the elastic modulus of each resultant PAG was confirmed by an indentation test using an atomic force microscope (AFM) with a sharp-tipped probe (BioScope Catalyst BioAFM, Billerica, MA, USA). For roughness calculations, AFM imaging was performed by using a Dimension 3100 (NanoscopeV; Bruker, Santa Barbara, CA, USA). Contact-mode topographic images were taken with an applied force maintained below 2 nN at a scan rate of 1 Hz

Table. Immunochemical and Cytochemical Markers

Marker	Indicative of
Vinculin	Focal adhesions
Phalloidin	Actin
DAPI	Nuclei
GFAP	Müller cell component; Müller cell activation
CRALBP	Müller cell differentiation
α-SMA	Müller cell component; component of stress fibers

(Supplementary Fig. S1). Si3N4 cantilevers (Bruker) with a spring constant of 0.06 N/m (according to manufacturer specifications) were used. Roughness (R_a) was calculated by using the NanoScope Analysis software (V1.6) from Bruker, using the following formula:

$$R_a = \frac{1}{N}\sum_{j=1}^{N}|Z_j|.$$

In addition, R_{max} values representing the maximum vertical distance between the highest and lowest data points in the image following the planefit were calculated.

Cell Seeding and Morphology

MIO-M1 cells were seeded onto the PAGs (5×10^4/cm^2) in the 6-well plates and allowed to grow in the cell culture incubator for 24 hours at 37°C with 5% CO_2. Experiments were done in triplicates. Afterwards, the cells were assessed by indirect fluorescence immunocytology (see below). Cells reached 90% confluence after 72 hours of incubation.

The Responsiveness of MIO-M1 Cells Grown on Different Elastic Moduli to TGF-β1 and TGF-β2

The effects of TGF-β1 or TGF-β2 administration on the expression of α-SMA in MIO-M1 cells seeded onto PAGs of varying elastic moduli (2, 4, 12, 26, and 92 kPa) were studied. The coverslips without PAGs that underwent the entire cross-linking and type I collagen–coating procedure were used as a control group. MIO-M1 cells were seeded onto the PAGs (5×10^4/cm^2) in 6-well plates and allowed to adhere in stock medium containing 10% FBS for 24 hours at 37°C with 5% CO_2. Afterwards, MIO-M1 cells were treated with recombinant TGF-β1 or TGF-β2 (10 ng/mL[6]; R&D Systems, Minneapolis, MN, USA) or PBS, which was used as a negative control. After 48 hours of incubation in a cell culture incubator, the MIO-M1 cells were collected for immunocytologic analysis.

Indirect Fluorescence Immunocytology

The MIO-M1 cells were briefly rinsed in PBS and fixed with 1:1 acetone/methanol at −20°C for 10 minutes. The cells were then rinsed with PBS and preincubated in 5% bovine serum albumin (BSA; Sanquin, Amsterdam, The Netherlands) in PBS to block unspecific binding, and then incubated with primary antibodies diluted 1:100 in PBS. For the analysis of focal adhesions and the actin cytoskeleton, the cells were first incubated in mouse anti-vinculin antibody (diluted to 1:100 in PBS; Sigma-Aldrich Corp.) for an hour, followed by incubation in fluorescein-isothiocyanate (FITC)–conjugated donkey anti-mouse antibody (green, to stain focal adhesions), tetramethylrhodamine B isothiocyanate (TRITC)–conjugated phalloidin (red, to stain the actin filaments), and 4′,6-diamidino-2-phenylindole (DAPI, blue, for nuclear counterstaining, 1:200; Sigma-Aldrich Corp.) for another hour. The entire staining procedure was performed in a dark chamber at room temperature. The phalloidin-stained area representing the actin of the cytoskeleton was measured on images obtained by confocal laser scanning microscopy (CLSM, Leica TCS-SP2; Leica, Wetzlar, Germany) using ImageJ software (http://imagej.net; provided in the public domain by the National Institutes of Health, Bethesda, MD, USA) and taken as a measure for the cell surface area; the average cell surface areas were calculated from at least 50 cells from nine images in total of three independent experiments.

For protein expression analysis, primary antibodies of different producers (usually mouse and rabbit) were combined. The primary antibodies used included mouse anti-GFAP antibody (GFAP, marker of Müller cell activation; Sigma-Aldrich Corp.); rabbit anti-CRALBP antibody (CRALBP, UW55, a kind gift from John C. Saari; University of Washington, Seattle, WA, USA); and mouse anti–α-SMA (Sigma-Aldrich Corp.; Table). The cells were fixed with 1:1 acetone/methanol and then incubated in 5% BSA, as aforementioned. Then, the cells were incubated in a mixture of two primary antibodies (both were diluted to 1:100 in PBS) for 1 hour at room temperature. Afterwards, the cells were rinsed with PBS and incubated in secondary antibodies with fluorescent conjugations for 1 hour in a dark chamber at room temperature. Depending on the species that produced the primary antibody, the following secondary antibodies were included: FITC-conjugated donkey anti-mouse antibody, and TRITC-conjugated donkey anti-rabbit antibody (1:200; Jackson ImmunoResearch Laboratories, Inc., West Grove, PA, USA). Nucleus counterstaining was performed by using DAPI (1:200; Sigma-Aldrich Corp.). After staining, the cells on the PAG-coated coverslips were placed on slides with a drop of antifadent (AF1; Citifluor Ltd., London, UK) and sealed. The entire immunocytologic procedures were performed at room temperature under dark conditions.

Photodocumentation and Statistical Analysis

A fluorescence microscope (Leica DMR) and CLSM (Leica) were used to document the samples. ImageJ software was used to manually mark cell borders and calculate cell numbers and cell surface areas.

The data were analyzed by SigmaPlot 12.1 (Systat Software, Inc., San Jose, CA, USA). Because the data of cell surface area values were not normally distributed, Kruskal-Wallis 1-way analysis of variance on ranks and Dunn's post hoc method were used to compare the groups. $P < 0.05$ was considered statistically significant.

Results

Substrate Elasticity Modulates the Cell Surface Area of MIO-M1 Cells

At the start of each experiment, MIO-M1 cells were checked for and found to express CRALBP and α-SMA in a diffuse pattern, with only very limited amounts of GFAP (Fig. 1A–C). The MIO-M1 cells, plated on PAGs with different elastic moduli, displayed different morphologic features, including cell surface area, organization of intracellular actin fibers, and expression of vinculin in focal adhesions and cytoplasm (Figs. 2, 3).

A gradual increase in surface area of the MIO-M1 cells was observed, along with increasing elastic modulus of the PAGs between 2 and 26 kPa (Fig. 2). At values higher than 26 kPa, the median of the cell surface areas of MIO-M1 cells remained stable (Fig. 2). Statistical analysis showed that cells grown on 2-kPa PAGs had a smaller surface area than those grown on 4-, 12, 26-, and 92-kPa PAGs, and on control coverslips ($P < 0.001$).

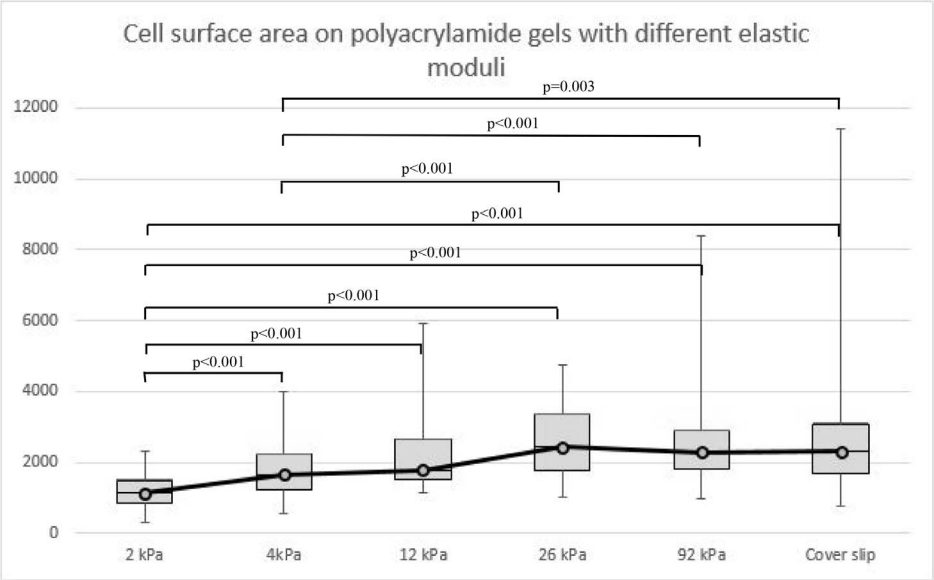

Cell surface area (μm^2)	2 kPa	4 kPa	12 kPa	26 kPa	92 kPa	Cover slip
Minimum	320,77	549,17	1141,01	1032,81	977,28	754,44
First quartile	865,83	1230,98	1517,64	1783,81	1812,72	1699,09
Median	1138,74	1665,00	1786,09	2432,06	2286,31	2314,43
Third quartile	1483,93	2216,95	2646,06	3345,78	2895,93	3070,09
Maximum	2330,91	3998,77	5923,39	4753,54	8386,43	11386,59

Figure 2. *Box plots* showing cell surface area (μm^2) of MIO-M1 cells on PAGs with different elastic moduli. MIO-M1 cells were seeded on PAG-coated or control coverslips for 24 hours. With increasing stiffness of the PAGs, a trend of gradual increase in cell surface area was observed, which reached its maximum at 26 kPa. The median of the cell surface area on 2-kPa PAGs was significantly smaller than that on 4-, 12-, 26-, and 92-kPa PAGs, and coverslip ($P < 0.001$). Cells grown on 4-kPa PAGs had a smaller surface area than those grown on 26- and 92-kPa PAGs ($P < 0.001$), and coverslip ($P = 0.003$). The difference between 4 and 12 kPa and the differences between 12, 26, 92 kPa and coverslip were not statistically significant. *Error bars*: Minimal and maximal value of the cell surface area. *Square bar*: First and third quartiles. *Dots in the bar*: Median.

Cells grown on 4-kPa PAGs had a smaller surface area than those grown on 26- and 92-kPa PAGs ($P < 0.001$), and coverslip ($P = 0.003$) (Fig. 2). The difference between 4 and 12 kPa, and the differences between 12, 26, 92 kPa, and coverslip were not statistically significant.

Substrate Elasticity Modulates Cytoskeleton Organization and Focal Adhesions of MIO-M1 Cells

We observed a clear relationship between increasing elastic modulus of the PAGs and cell morphology (Fig. 3). Phalloidin staining showed that actin was present in all cells, mainly in filaments. Filaments were not observed in a few of the single cells grown on 2-kPa PAGs. However, single cells were scarce, since the cells usually formed clusters with cell–cell contact after 24 hours of adhesion. Cells organized in clusters were often elongated and contained prominent actin filaments (Fig. 3A). Actin filaments in MIO-M1 cells grown on 2- and 4-kPa PAGs were relatively thin and less organized than those in cells grown on the stiffer substrates. MIO-M1 cells grown on 12-, 26, and 92-kPa PAGs formed prominent stress fibers (Fig. 3A). Vinculin staining also showed clear differences in cell morphology in relation to substrate stiffness (Fig. 3B); focal adhesions in MIO-M1 on softer PAGs (2 and 4 kPa) were visible as small dot-like structures approximately 1 μm in length, which would correspond to focal complexes. These small dot-like structures were randomly distributed over the cell-surface contact area. In addition, prominent intracytoplasmic vinculin immunopositivity in MIO-M1 cells on soft PAGs (2 and 4 kPa) was seen, indicating vinculin that was not incorporated into focal adhesions (Fig. 3B). In contrast, focal adhesions on stiffer PAGs (12, 26, and 92 kPa) had the typical morphologic features of mature focal adhesions as described by Riveline and coworkers.[32] They formed 2- to 5-μm-long structures, which were intensely stained by anti-vinculin antibodies and colocalized with the distal endings of the stress fibers at sites of cell–matrix adhesions (Fig. 3B).

Substrate Elasticity Modulates the Intracellular Organization of α-SMA Stress Fibers in TGF-β–Treated MIO-M1 Cells

We investigated the effect of substrate elasticity on both TGF-β1– and TGF-β2–induced α-SMA stress fiber expression in MIO-M1 cells. In cells grown on softer PAGs (2 and 4 kPa), diffuse intracytoplasmic α-SMA positivity was observed, whereas α-SMA stress fibers were not prominent. In cells grown on more rigid surfaces in the presence of TGF-β, prominent α-SMA stress fibers were seen. These stress fibers were observed as straight fibers aligned with the long axis of the cells (Figs. 4, 5).

Discussion

To explore the role of substrate stiffness in regulating the morphology and function of retinal Müller cells, we studied the cytoskeletal morphology and formation of focal adhesion in

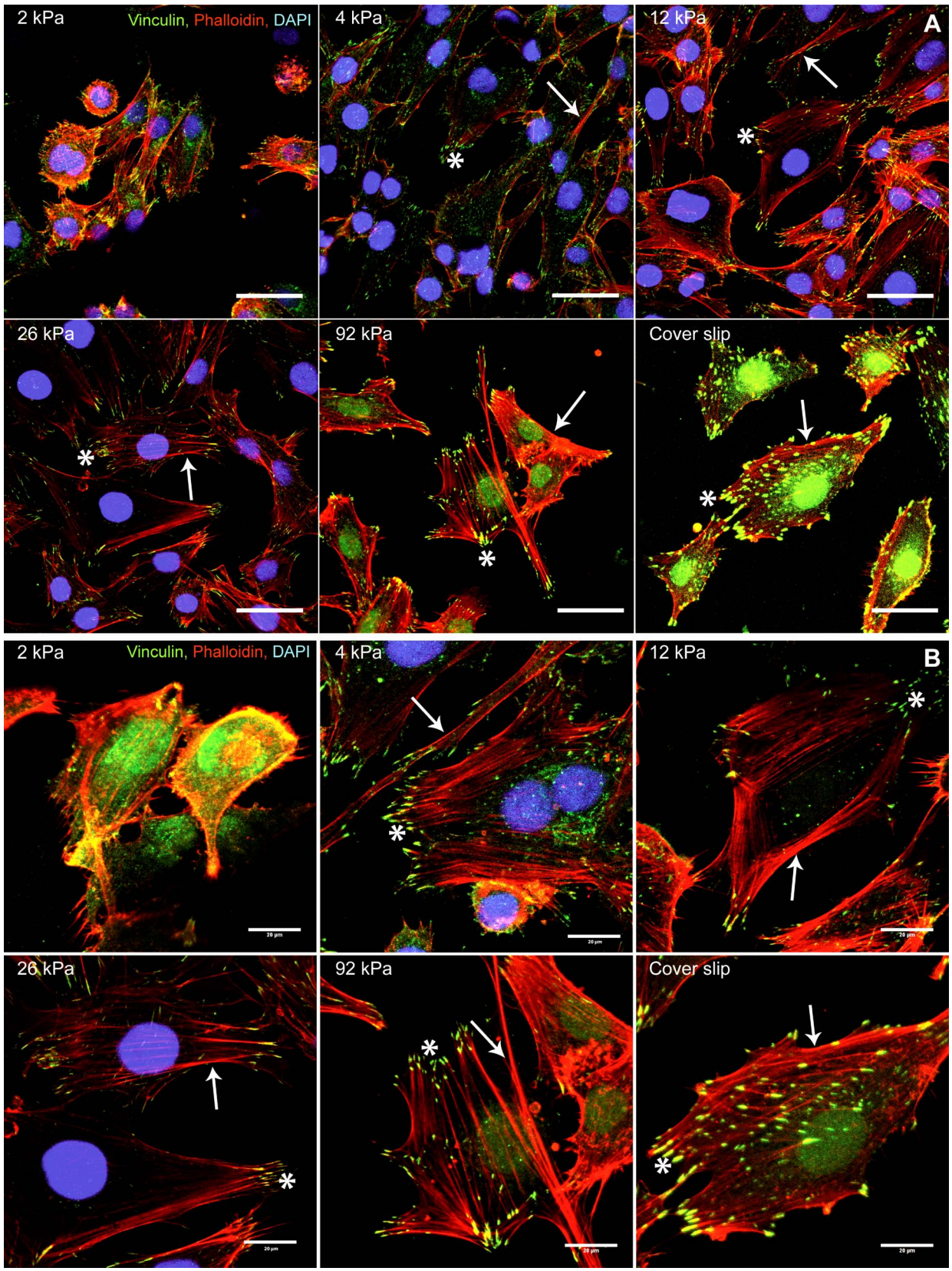

Figure 3. Confocal scanning laser microscopy images of cytoskeleton and focal adhesions of MIO-M1 cells on PAGs with different elastic moduli. MIO-M1 cells were seeded on PAGs with different elastic moduli (ranging from 2–92 kPa and coverslips with the same surface coating) and cultured for 24 hours. The cells were stained with vinculin antibodies (indicating focal adhesions; *green*, *asterisks*) and phalloidin to stain actin filaments (*red*, *arrows*). Nuclei were counterstained with DAPI (*blue*). (**A**) Single cells without and cell clusters with thin actin filaments in cells grown on soft PAGs (2 and 4 kPa). Prominent stress fibers spanning the entire cell in cells grown on stiffer PAGs (12–92 kPa and coverslip). Vinculin staining displayed small dot-like structures in cells grown on soft PAGs (2 and 4 kPa), corresponding to focal complexes. On stiffer PAGs, larger and elongated focal adhesions were present. Furthermore, cells on soft PAGs contained intracytoplasmic vinculin, indicating a dynamic vinculin assembly or dissociation from the focal adhesion. In some images, the *blue* DAPI staining could not be visualized owing to technical problems with the microscope. In those instances, cell nuclei can be recognized by their oval shape and *green* color. *Scale bars*: 50 μm. (**B**) Upon higher magnification, the vinculin-containing focal adhesions on rigid PAGs (12–92 kPa and control coverslips) had the classical aspect of mature focal adhesions, whereas focal adhesions on soft PAGs were small dot-like focal complexes. On 2–12–92 kPa and coverslip, the DAPI staining was omitted. *Scale bars*: 20 μm.

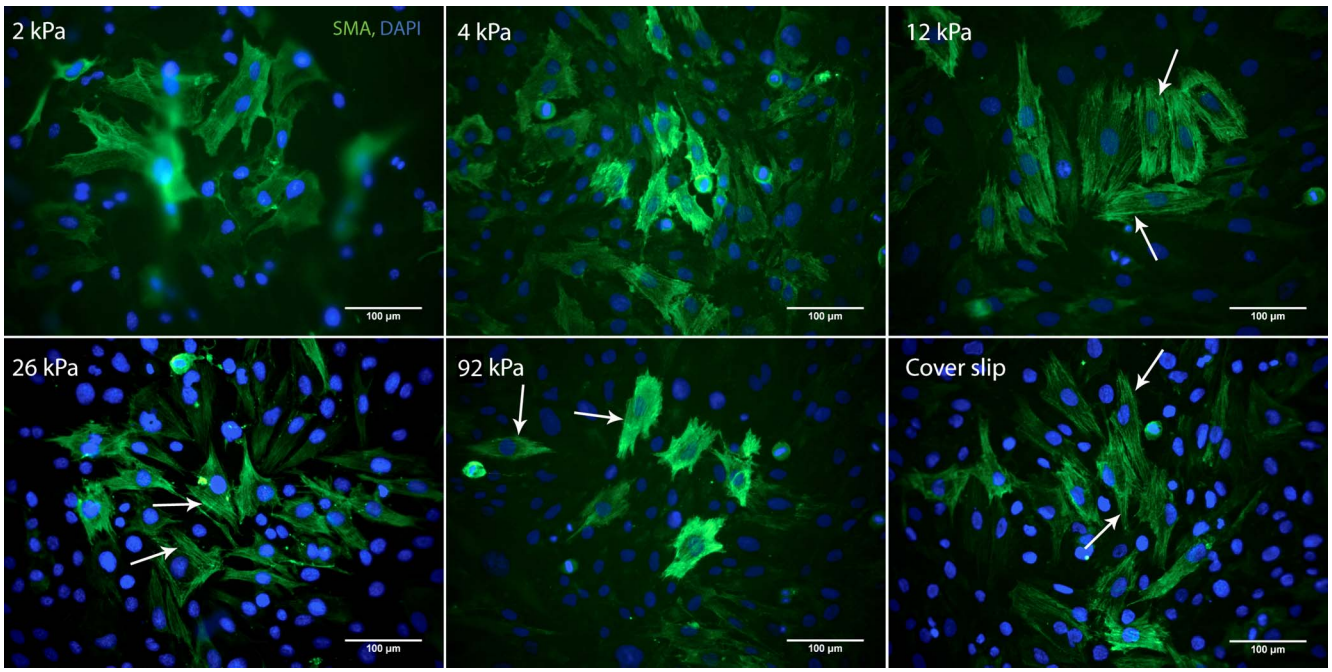

Figure 4. Transforming growth factor-β1 induced α-SMA stress fibers in MIO-M1 cells grown on PAGs with different elastic moduli. MIO-M1 cells were seeded on PAGs with different elastic moduli ranging from 2 to 92 kPa or on rigid polystyrene (coverslip), stimulated with TGF-β1 for 48 hours and stained for α-SMA (*green*). Stress fibers are indicated by *arrows*. The nuclei were counterstained with DAPI (*blue*). *Scale bars*: 100 μm.

retinal Müller cells grown on PAGs with different elastic moduli. In addition, our results showed that the elastic modulus of the substrate affects the TGF-β1– and TGF-β2–induced expression of α-SMA and its incorporation into stress fibers.

Our experiments indicate that retinal Müller cells are mechanosensitive by showing that the elastic modulus of the substrate influenced their actin cytoskeletal morphology and focal adhesions. Cytoskeletal organization and the formation of mature focal adhesions were prominent in cells grown on PAGs

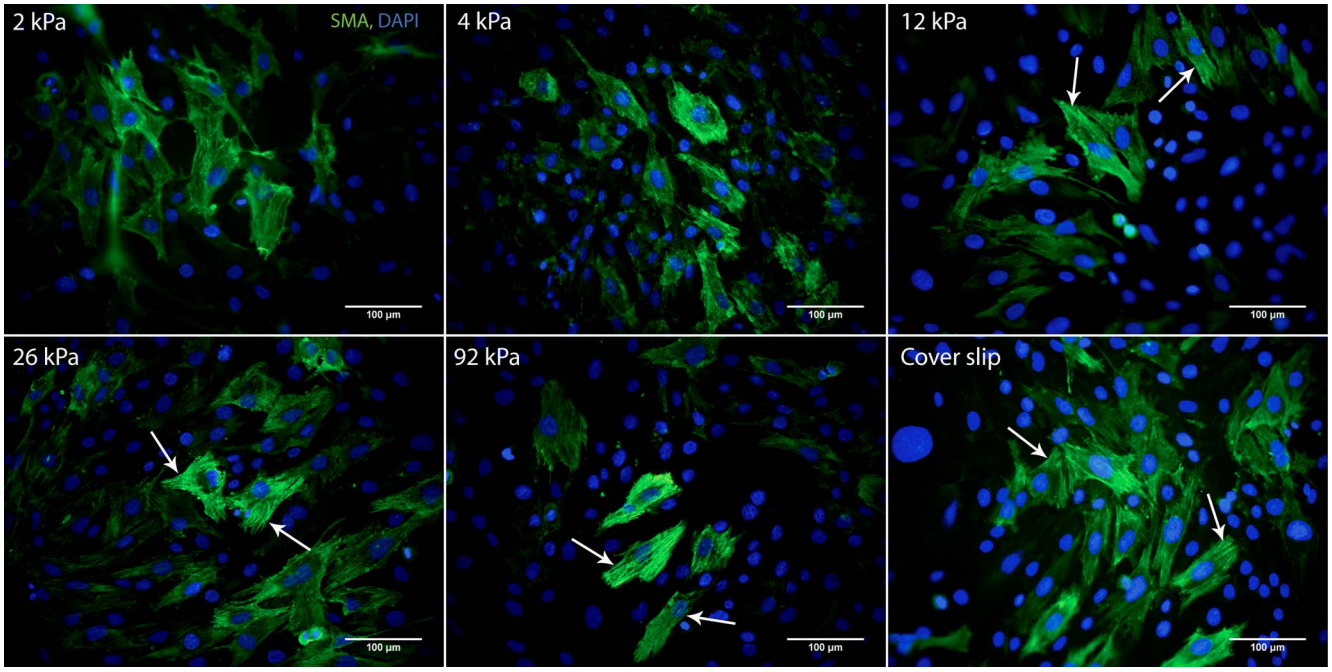

Figure 5. Transforming growth factor-β2 induced α-SMA stress fibers in MIO-M1 cells grown on PAGs with different elastic moduli. MIO-M1 cells were seeded on PAGs with different elastic moduli ranging from 2 to 92 kPa, stimulated with TGF-β2 for 48 hours, and stained for α-SMA (*green*). Stress fibers are indicated by *arrows*. The nuclei were counterstained with DAPI (*blue*). *Scale bars*: 100 μm.

Investigative Ophthalmology & Visual Science

of 12 kPa and more, whereas cell surface areas reached their maximum on 26-kPa PAGs. The most striking differences were found between the soft PAGs (2 and 4 kPa) versus all the stiffer PAGs (12 kPa and higher). A possible explanation for this may be that cells can only be stimulated up to a certain maximum. After that, further stimulation will no longer have an additive effect.

Most cells not only respond to mechanical forces but actively probe substrate flexibility by applying contractile forces through focal adhesions and by responding to the feedback of counterforce.[33,34] An increasing number of cellular processes, such as cell spreading, cytoskeletal remodeling, and adhesion, have been found to depend on mechanical cues originating from the extracellular microenvironment.[34] Epithelial cells and fibroblasts are the first cell types reported to respond differently to soft versus rigid substrates.[28] Since then, various cell types have been shown to exhibit different sensitivities in response to the elastic modulus of the surrounding matrix.[35,36] For example, neurons are reported to prefer soft substrates with an elastic modulus of less than 1 kPa.[37,38] Previous studies already have suggested that retinal Müller cells are mechanosensitive,[22] since they can respond to external forces (outside-in) such as cyclic traction by changing their protein expression profile and function.[39,40] The morphologic aspects of Müller cells in relation to substrate stiffness as observed in our study—including smaller cell surface areas, and less organized cytoskeletons and stress fibers on soft as compared to stiff substrates—are consistent with prior experiments by others on fibroblasts, epithelial cells, astrocytes, and Müller cells. For example, a clear relationship between more prominent actin stress fibers and an increase in cell surface area in fibroblasts grown on stiffer surfaces has been described by Yeung et al.[35] Since different cell types respond to the substrate's stiffness, and adapt their morphologic and functional activities differently, substrate elasticity should be taken into consideration when cellular behavior of Müller cells is studied.[25,35]

We observed significant differences in cellular morphology between the Müller cells grown on soft PAGs (2 and 4 kPa) and stiffer substrates (12- to 92-kPa PAGs and control coverslip). Similar morphologic differences have been reported in a mouse Müller cell culture study using PAGs.[25] We furthered the previous observation in the present human cell model by defining the threshold of elasticity at which the stress fibers—containing actin filaments and focal adhesions that contain vinculin in the Müller cells—start to be prominently expressed. The threshold for Müller cells was between 4 and 12 kPa, which is similar to the threshold found in fibroblasts. When substrate stiffness was more than 9 kPa, fibroblasts switched from being round and having a lack of stress fibers to the typical fibroblast seen in conventional tissue cultures, with abundant stress fibers and elongated focal adhesions.[35] The mechanism proposed entails the substrate stiffness being higher than the elastic modulus of the fibroblast itself, which allows the internal contractile forces to result in a deformation not only of the external matrix but also of the cytoskeleton.[35]

We observed that the increase in incorporation of actin filaments into the cytoskeleton, the maturation of focal adhesions, and the vinculin recruitment were coincident with an increase in substrate stiffness. These findings indicate that the substrate elasticity has an impact on focal adhesion and actin cytoskeleton formation, which result in changes in Müller cell dynamics and morphology. The focal adhesion, which links the extracellular matrix and actin cytoskeleton, has been shown to be one of the important surface-sensing "organelles."[41] The initiation and growth of focal adhesions are strongly dependent on the tension of the actin filaments they are tethered to.[42] Vinculin is one of the important intracellular, mechanosensing molecules among the protein components of the complex focal adhesion.[43] The observed differences in vinculin staining in cells on soft substrates (diffuse cytoplasmatic) and cells on stiff substrates (present in focal adhesions) is consistent with previous observations in other cell types, which suggests that the recruitment and maintenance of vinculin in focal adhesions are both regulated by tension.[28] Lee and coworkers[44] have demonstrated that the local tensile force could induce the exposure of the major vinculin binding site on talin, which is the core protein that interacts with vinculin in the focal adhesion. Carisey and coworkers[45] have shown that vinculin is dissociated from the focal adhesions, when the local actomyosin-mediated tension is disrupted by Rho-associated protein kinase inhibitor. It has been previously shown that the compliance of the soft substrate interferes with the feedback loop that interconnects the formation of focal adhesions and polymerization of the actin cytoskeleton, resulting in the dissociation of vinculin from the focal adhesion and the disruption of the actin cytoskeleton. Our observation of diffuse intracellular vinculin staining in cells grown on soft PAGs is in line with this. Previous studies[46,47] have shown that vinculin stabilizes the focal adhesion and promotes focal adhesion growth with increasing tension. Therefore, our observation indicates that vinculin is actively involved in the mechanosensitivity of Müller cells.

The link between mechanical strain and fibrosis is clinically well established.[48] Our observations demonstrated a clear influence of the mechanical environment on the organization of α-SMA in stress fibers in retinal Müller cells, which is consistent with previous reports in fibroblasts.[9,49] The administration of TGF-β for 48 hours induced prominent α-SMA stress fiber formation in retinal Müller cells on stiff PAGs, while the expression of α-SMA was less significant and the α-SMA stress fibers were disorganized in the Müller cells on soft PAGs. These findings would be consistent with the hypothesis that retinal Müller cells, which migrate from the soft intraretinal environment onto the inner limiting membrane (ILM), will thus encounter a stiffer environment. The stiffer ILM influences cell morphology and the expression of proteins within the Müller cell, contributing to changing the Müller cell phenotype toward a myofibroblast-like phenotype. This process is further enhanced by TGF-β, whose presence is increased in iERM.[12] The myofibroblast-like cells will contribute to the initial stages of fibrosis by collagen formation and deposition. Newly formed collagens in combination with the presence of myofibroblasts will promote tissue contraction, further fibrosis, and thus increase tissue stiffness.[50,51] This will provide an even more rigid surface for the Müller cells, which may be a factor in promoting advanced fibrosis. While both TGF-β and surface stiffness may thus contribute to the process of fibrosis, the factor that initially triggers Müller cell migration remains unknown.

An experimental animal model of ERM formation has shown that vinculin and α-SMA expression are significantly increased in Müller cells that reside in the ERM, compared to that of Müller cells in the retina.[22] It is conceivable that the increased stiffness of retinal fibrotic tissue could provide an extracellular microenvironment that promotes the upregulation of α-SMA in retinal Müller cells, resulting in further fibrosis and contraction.

The tunable collagen-coated PAG culture system could perhaps be used as a model to mimic the differences in tissue stiffness that Müller cells may encounter in their in vivo environments during physiological and pathologic processes. Since substrate elasticity has been recognized as one of the crucial biomechanical factors that regulate the morphology, migration, proliferation, and transdifferentiation of mammalian

cells,[35,52] several types of hydrogels, including collagen matrix, matrigel, agarose, and others, have been applied as environmental models.[53,54] The major drawbacks of these biological polymers is that their different elastic moduli are controlled by varying the concentration of collagen, which also results in significant differences in the mesh sizes of the gels.[55] The collagen-coated PAG system has been developed to overcome some of the aforementioned problems. The elastic moduli of the PAGs can be manipulated by varying the ratio of acrylamide and bisacrylamide without changing the surface chemistry and texture.[56] Furthermore, the PAGs are biochemically stable materials, which provides an opportunity to study the effect of elastic modulus on cell behavior on chemically identical surfaces.[56]

The use of a cell culture model has several advantages but also drawbacks. Advantages include the possibility of studying the effects of individual variables, for example, surface stiffness and TGF-β. Obvious limitations include the use of an in vitro system, isolated cells, and a completely artificial environment. Thus, findings will only serve to formulate hypotheses on the in vivo situation, while firm conclusions cannot be drawn. The MIO-M1 cell line we used has the advantage of being a spontaneously immortalized human Müller cell line that has been thoroughly characterized.[27] It has been observed to retain important characteristics of Müller cells in situ.[27] A striking difference with Müller cells in situ is the expression of α-SMA, which has not been reported in Müller cells in situ or freshly isolated (primary) Müller cells.[16,22] Guidry and coworkers,[16] using primary human retinal Müller cells, have found that the expression of α-SMA is not prominent until 14 days of culture, whereas α-SMA positivity and the presence of α-SMA stress fibers increase with an increasing number of passages. Under standard cell culture conditions, cells are grown on rigid surfaces, which stimulate phenotype alterations.[16,22,27,57] The soft PAGs, as used in the present study, may provide a means to prevent this.

Summary and Perspective

Cells constantly exert tractional forces on their extracellular matrix through their actin filaments and focal adhesions. The elasticity of the extracellular matrix will determine the feedback force, which can be sensed by the cells through their focal adhesions, which in turn can trigger certain general intracellular processes resulting in changes in cellular functions. Understanding the underlying molecular mechanisms of mechanotransduction in the retinal Müller cell may provide new treatment strategies in the prevention of retinal fibrocontractive diseases. The development of an in vitro model to simulate both the normal compliant retinal tissue and the rigid retinal fibrotic tissue may provide additional knowledge to fill the gap between the results of cell cultures performed in traditional petri dishes with rigid surfaces and in vivo findings.

Acknowledgments

We thank Nomdo M. Jansonius from the Department of Ophthalmology for his advice on statistical analysis. We are grateful for the help of Joop de Vries from the Department of Biomedical Engineering with the indentation testing using the atomic force microscope.

Supported by Stichting Blindenhulp, The Netherlands.

Disclosure: **S.-C. Bu**, None; **R. Kuijer**, None; **R.J. van der Worp**, None; **S.M. van Putten**, None; **O. Wouters**, None; **X.-R. Li**, None; **J.M.M. Hooymans**, None; **L.I. Los**, None

References

1. Pastor JC, de la Rua ER, Martin F. Proliferative vitreoretinopathy: risk factors and pathobiology. *Prog Retin Eye Res*. 2002; 21:127–144.
2. Guidry C. The role of Muller cells in fibrocontractive retinal disorders. *Prog Retin Eye Res*. 2005;24:75–86.
3. Tosi GM, Marigliani D, Romeo N, Toti P. Disease pathways in proliferative vitreoretinopathy: an ongoing challenge. *J Cell Physiol*. 2014;229:157715–83.
4. Gabbiani G. The myofibroblast in wound healing and fibrocontractive diseases. *J Pathol*. 2003;200:500–503.
5. George SJ. Regulation of myofibroblast differentiation by convergence of the Wnt and TGF-beta1/Smad signaling pathways. *J Mol Cell Cardiol*. 2009;46:610–611.
6. Shi Y, Dong Y, Duan Y, Jiang X, Chen C, Deng L. Substrate stiffness influences TGF-beta1-induced differentiation of bronchial fibroblasts into myofibroblasts in airway remodeling. *Mol Med Rep*. 2013;7:419–424.
7. Guvendiren M, Perepelyuk M, Wells RG, Burdick JA. Hydrogels with differential and patterned mechanics to study stiffness-mediated myofibroblastic differentiation of hepatic stellate cells. *J Mech Behav Biomed Mater*. 2014;38:198–208.
8. Galie PA, Westfall MV, Stegemann JP. Reduced serum content and increased matrix stiffness promote the cardiac myofibroblast transition in 3D collagen matrices. *Cardiovasc Pathol*. 2011;20:325–333.
9. Meyer-ter-Vehn T, Han H, Grehn F, Schlunck G. Extracellular matrix elasticity modulates TGF-beta-induced p38 activation and myofibroblast transdifferentiation in human tenon fibroblasts. *Invest Ophthalmol Vis Sci*. 2011;52:9149–9155.
10. Hoerster R, Muether PS, Vierkotten S, Hermann MM, Kirchhof B, Fauser S. Upregulation of TGF-ss1 in experimental proliferative vitreoretinopathy is accompanied by epithelial to mesenchymal transition. *Graefes Arch Clin Exp Ophthalmol*. 2014;252:11–16.
11. Kon CH, Occleston NL, Aylward GW, Khaw PT. Expression of vitreous cytokines in proliferative vitreoretinopathy: a prospective study. *Invest Ophthalmol Vis Sci*. 1999;40:705–712.
12. Iannetti L, Accorinti M, Malagola R, et al. Role of the intravitreal growth factors in the pathogenesis of idiopathic epiretinal membrane. *Invest Ophthalmol Vis Sci*. 2011;52: 5786–5789.
13. Jones IL, Warner M, Stevens JD. Mathematical modelling of the elastic properties of retina: a determination of Young's modulus. *Eye*. 1992;6(pt 6):556–559.
14. Lu YB, Iandiev I, Hollborn M, et al. Reactive glial cells: increased stiffness correlates with increased intermediate filament expression. *FASEB J*. 2011;25:624–631.
15. Guidry C. Isolation and characterization of porcine Muller cells: myofibroblastic dedifferentiation in culture. *Invest Ophthalmol Vis Sci*. 1996;37:740–752.
16. Guidry C, Bradley KM, King JL. Tractional force generation by human muller cells: growth factor responsiveness and integrin receptor involvement. *Invest Ophthalmol Vis Sci*. 2003;44: 1355–1363.
17. Kohno RI, Hata Y, Kawahara S, et al. Possible contribution of hyalocytes to idiopathic epiretinal membrane formation and its contraction. *Br J Ophthalmol*. 2009;93:1020–1026.
18. Ma J, Zhang Q, Moe MC, Zhu T. Regulation of cell-mediated collagen gel contraction in human retinal pigment epithelium cells by vascular endothelial growth factor compared with transforming growth factor-beta2. *Clin Experiment Ophthalmol*. 2012;40:e76–e86.
19. Guidry C, King JL, Mason JO III. Fibrocontractive Muller cell phenotypes in proliferative diabetic retinopathy. *Invest Ophthalmol Vis Sci*. 2009;50:1929–1939.

20. Bringmann A, Wiedemann P. Involvement of Muller glial cells in epiretinal membrane formation. *Graefes Arch Clin Exp Ophthalmol*. 2009;247:865–883.
21. Bunt-Milam AH, Saari JC. Immunocytochemical localization of two retinoid-binding proteins in vertebrate retina. *J Cell Biol*. 1983;97:703–712.
22. Isiksoy S, Basmak H, Kasapoglu Dundar E, Ozer A. Expression of proteins associated with cell-matrix adhesion in proliferative vitreoretinopathy designed by Dispase model. *Eur J Ophthalmol*. 2007;17:89–103.
23. Fisher SK, Lewis GP. Muller cell and neuronal remodeling in retinal detachment and reattachment and their potential consequences for visual recovery: a review and reconsideration of recent data. *Vis Res*. 2003;43:887–897.
24. Candiello J, Cole GJ, Halfter W. Age-dependent changes in the structure, composition and biophysical properties of a human basement membrane. *Matrix Biol*. 2010;29:402–410.
25. Davis JT, Wen Q, Janmey PA, Otteson DC, Foster WJ. Muller cell expression of genes implicated in proliferative vitreoretinopathy is influenced by substrate elastic modulus. *Invest Ophthalmol Vis Sci*. 2012;53:3014–3019.
26. Lindqvist N, Liu Q, Zajadacz J, Franze K, Reichenbach A. Retinal glial (Muller) cells: sensing and responding to tissue stretch. *Invest Ophthalmol Vis Sci*. 2010;51:1683–1690.
27. Limb GA, Salt TE, Munro PM, Moss SE, Khaw PT. In vitro characterization of a spontaneously immortalized human Muller cell line (MIO-M1). *Invest Ophthalmol Vis Sci*. 2002; 43:864–869.
28. Pelham RJ Jr, Wang Y. Cell locomotion and focal adhesions are regulated by substrate flexibility. *Proc Natl Acad Sci U S A*. 1997;94:13661–13665.
29. Wang YL, Pelham RJ Jr. Preparation of a flexible, porous polyacrylamide substrate for mechanical studies of cultured cells. *Methods Enzymol*. 1998;298:489–496.
30. Wollensak G, Spoerl E. Biomechanical characteristics of retina. *Retina*. 2004;24:967–970.
31. Henrich PB, Monnier CA, Halfter W, et al. Nanoscale topographic and biomechanical studies of the human internal limiting membrane. *Invest Ophthalmol Vis Sci*. 2012;53:2561–2570.
32. Riveline D, Zamir E, Balaban NQ, et al. Focal contacts as mechanosensors: externally applied local mechanical force induces growth of focal contacts by an mDia1-dependent and ROCK-independent mechanism. *J Cell Biol*. 2001;153:1175–1186.
33. Wang HB, Dembo M, Wang YL. Substrate flexibility regulates growth and apoptosis of normal but not transformed cells. *Am J Physiol Cell Physiol*. 2000;279:C1345–C1350.
34. Discher DE, Janmey P, Wang YL. Tissue cells feel and respond to the stiffness of their substrate. *Science*. 2005;310:1139–1143.
35. Yeung T, Georges PC, Flanagan LA, et al. Effects of substrate stiffness on cell morphology, cytoskeletal structure, and adhesion. *Cell Motil Cytoskeleton*. 2005;60:24–34.
36. Engler A, Bacakova L, Newman C, Hategan A, Griffin M, Discher D. Substrate compliance versus ligand density in cell on gel responses. *Biophys J*. 2004;86:617–628.
37. Flanagan LA, Ju YE, Marg B, Osterfield M, Janmey PA. Neurite branching on deformable substrates. *Neuroreport*. 2002;13: 2411–2415.
38. Georges PC, Miller WJ, Meaney DF, Sawyer ES, Janmey PA. Matrices with compliance comparable to that of brain tissue select neuronal over glial growth in mixed cortical cultures. *Biophys J*. 2006;90:3012–3018.
39. Wang X, Fan J, Zhang M, Sun Z, Xu G. Gene expression changes under cyclic mechanical stretching in rat retinal glial (Muller) cells. *PLoS One*. 2013;8:e63467.
40. Miller WJ, Leventhal I, Scarsella D, Haydon PG, Janmey P, Meaney DF. Mechanically induced reactive gliosis causes ATP-mediated alterations in astrocyte stiffness. *J Neurotrauma*. 2009;26:789–797.
41. Geiger B, Spatz JP, Bershadsky AD. Environmental sensing through focal adhesions. *Nat Rev Mol Cell Biol*. 2009;10:21–33.
42. Gerthoffer WT, Gunst SJ. Invited review: focal adhesion and small heat shock proteins in the regulation of actin remodeling and contractility in smooth muscle. *J Appl Physiol*. 2001;91: 963–972.
43. Galbraith CG, Yamada KM, Sheetz MP. The relationship between force and focal complex development. *J Cell Biol*. 2002;159:695–705.
44. Lee SE, Kamm RD, Mofrad MR. Force-induced activation of talin and its possible role in focal adhesion mechanotransduction. *J Biomech*. 2007;40:2096–2106.
45. Carisey A, Tsang R, Greiner AM, et al. Vinculin regulates the recruitment and release of core focal adhesion proteins in a force-dependent manner. *Curr Biol*. 2013;23:271–281.
46. Saunders RM, Holt MR, Jennings L, et al. Role of vinculin in regulating focal adhesion turnover. *Eur J Cell Biol*. 2006;85: 487–500.
47. Spanjaard E, de Rooij J. Mechanotransduction: vinculin provides stability when tension rises. *Curr Biol*. 2013;23: R159–R161.
48. Carver W, Goldsmith EC. Regulation of tissue fibrosis by the biomechanical environment. *BioMed Res Int*. 2013;2013: 101979.
49. Chia HN, Vigen M, Kasko AM. Effect of substrate stiffness on pulmonary fibroblast activation by TGF-beta. *Acta Biomater*. 2012;8:2602–2611.
50. Hinz B. The myofibroblast: paradigm for a mechanically active cell. *J Biomech*. 2010;43:146–155.
51. Horiguchi M, Ota M, Rifkin DB. Matrix control of transforming growth factor-beta function. *J Biochem*. 2012;152:321–329.
52. Ataollahi F, Pramanik S, Moradi A, et al. Endothelial cell responses in terms of adhesion, proliferation, and morphology to stiffness of polydimethylsiloxane elastomer substrates. *J Biomed Mater Res A*. 2015;103:2203–2213.
53. Plant AL, Bhadriraju K, Spurlin TA, Elliott JT. Cell response to matrix mechanics: focus on collagen. *Biochim Biophys Acta*. 2009;1793:893–902.
54. Reed J, Walczak WJ, Petzold ON, Gimzewski JK. In situ mechanical interferometry of matrigel films. *Langmuir*. 2009; 25:36–39.
55. Willits RK, Skornia SL. Effect of collagen gel stiffness on neurite extension. *J Biomater Sci Polym Ed*. 2004;15:1521–1531.
56. Georges PC, Janmey PA. Cell type-specific response to growth on soft materials. *J Appl Physiol*. 2005;98:1547–1553.
57. Hauck SM, Suppmann S, Ueffing M. Proteomic profiling of primary retinal Muller glia cells reveals a shift in expression patterns upon adaptation to in vitro conditions. *Glia*. 2003;44: 251–263.

Investigative Ophthalmology & Visual Science